Book of Tutorials and Abstracts

European Microbeam Analysis Society

EMAS 2023

17th

EUROPEAN WORKSHOP

on

MODERN DEVELOPMENTS AND APPLICATIONS IN MICROBEAM ANALYSIS

7 to 11 May 2023
at the
Jagiellonian University, Auditorium Maximum
Krakow, Poland

Under the auspices of the Rector of the
Jagiellonian University, Krakow, Poland
Organised in collaboration with the
Institute of Metallurgy and Materials Science of
the Polish Academy of Sciences, Krakow, Poland

EMAS
European Microbeam Analysis Society eV
www.microbeamanalysis.eu/

This volume is published by:
European Microbeam Analysis Society eV (EMAS)
EMAS Secretariat
c/o Eidgenössische Technische Hochschule, Institut für Geochemie und Petrologie
Clausiusstrasse 25
8092 Zürich
Switzerland

ISBN 978 90 8227 6961
NUR code: 972 – Materials Science

FOCUSSED BEAMS FOR USE IN EBSD

Bartłomiej Winiarski

Thermo Fisher Scientific, Materials & Structural Analysis
Pecha 12, 62700 Brno, Czech Republic
e-mail: bartlomiej.winiarski@thermofisher.com

Dr Bartlomiej (Bart) Winiarski is a staff scientist for Materials & Structural Analysis, Thermo Fisher Scientific, Brno, Czech Republic. He received his MSc in Materials Science from AGH - University of Science and Technology (Krakow, Poland), and holds a PhD in Mechanics of Composite Materials from the University of Aberdeen (Scotland). He received the R.E. Peterson Award from the Society of Experimental Mechanics (USA) in 2014 and has authored more than 30 peer-reviewed papers. From 2007 to 2013 he worked at the University of Manchester and National Physical Laboratory as post-doctoral researcher. From 2014 to 2016 he worked at the University of Manchester, Department of Materials, as FEI Research Fellow where he explored the application of Plasma Xe^+ FIB-SEM and metrological Helical Micro X-ray CT instruments to correlative multiscale/multimodal tomography in 3D materials science. He also developed novel methods for stress measurement at sub-micrometre scale using FIB-SEM and DIC techniques. In the period 2016-2020, he was a visiting academic at the University of Manchester, U.K.

1. ABSTRACT

Focussed beams (electrons, ions, and photons) are at the forefront of today's and future scientific and engineering advanced research instruments. The beams are typically used for six purposes: imaging, detection, deposition, implantation, milling/ablation, and polishing. There are plethora of detectable and useful signals coming from the beam irradiated matter. One of the signals is electron diffraction and scattering on a crystal planes used by electron backscatter diffraction (EBSD) method. This surface superficial probing technique is sensitive to surface contamination, amorphisation, and lattice distortions, thus requires damage-free sample surface preparation techniques. The advent of coupled multi-beam commercial instruments (DualBeams, CrossBeams and TriBeams) allowed for integration of sample surface preparation techniques, i.e., site specific (cross-sections, serial sections, thin lamellas, micro- and nano-pillars, etc.), and large areas (cross-sections and surface polishing), and beam excited signal detection/quantification methods, i.e., EBSD, EDS, WDS, SIMS, Raman, LIBS, etc. This paper attempts to bring closer the current state-of-the-art of focussed beams systems for use in EBSD technique in Materials Science.

2. HISTORICAL BRIEF ON DEVELOPMENT OF FOCUSSED BEAMS

Focussed beams are complex and compact systems that emit, accelerate, deflect, and raster a narrow stream of: (i) negatively charged particles - electrons, (ii) positively charged particles - ions, or (iii) photons. Currently these beams are typically used for six purposes: imaging, detection, deposition, implantation, milling/ablation, and polishing.

In the early days these devices formed a standalone analogue transmission electron microscope (TEM) [1, 2], scanning electron microscope (SEM) [3, 4], scanning ion microscope (SIM) (commercial systems based on liquid Ga^+ metal ion source (LMIS)) [5, 6], and light amplification by stimulated emission of radiation (LASER) (this is a very broad topic; here it is referred to low power < 10 W and pulsed lasers with impulse duration < 1 ns time domains, having application for low thermal or near-athermal material micro-machining, laser-induced signal measurements, e.g., laser-induced breakdown spectroscopy, and laser assisted material deposition) [7, 8], or short pulse (SPL) optics systems [9]. Currently, these standalone microscopes are based on digital circuits/logic systems. TEMs and SEMs evolved with improved electron sources, electron optics, aberration correctors, and various detection systems [10, 11]. SIM platforms range was extended with commercial scanning helium ion microscopes (SHIM) in 2008 [12] (also, neon is possible as primary ions), and xenon plasma FIB (PFIB) in 2011 [13]. Several experimental FIB sources are developed as well [14-16], e.g., liquid metal alloy ion sources (LMAIS), gas field ion sources (GFIS), low temperature ion sources (LOTIS), and magneto optical trap ion sources (MOTIS).

From the mid-2000's pulsed lasers and optics for fast micro-machining at sub-micrometre scale and *in situ* laser-based characterisation techniques have moved to ultra-short pulse lasers (UPL) (having a pulse duration < 1 ps, typically ~ 50 - 300 fs). These laser systems have capabilities of athermal and near damage-free ablation with the laser spot size of dozens of micrometres [18].

Circa the early 1990's the first systems with two columns emerged commercially [19]. These platforms have merged capabilities of SEM and focussed ion beam (FIB) column (based on liquid Ga^+ metal ions source - LMIS [5]), forming a single microscope with two beams defining a coincidence point (Fig. 1). In so doing a high-resolution electron imaging and qualitative detection modes of SEM (secondary electrons and backscattered electrons detection) are combined with implantation and milling/polishing mode of FIB. This configuration allows for site-specific micrometre-scale work, e.g., cross-sectioning, serial sectioning tomography, etc. [17]. Gradually, FIB-SEMs have been upgraded with analytical capabilities, e.g., energy-dispersive X-ray spectroscopy (EDS) and electron backscatter diffraction (EBSD) crystallographic data analysis. Automations of FIB-SEM routines led to development of 3D EBSD and 3D EDS methods (Fig. 2).

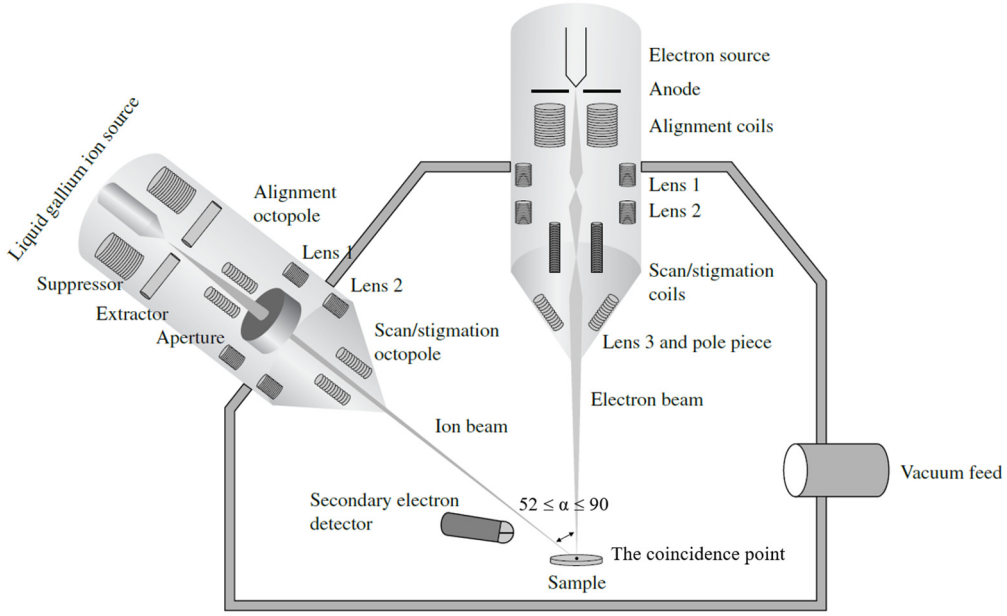

Figure 1. A schematic diagram is showing the configuration of two-beam focussed ion beam - scanning electron microscope system [17].

FIB at low beam currents (pA) can be focussed to a few nm spots sizes. However, the use of Ga^+ FIB column has two drawbacks:

a) Gallium can create low temperature eutectic alloys during ion matter interaction, particularly present along grain boundaries [21-23], e.g., in Fig. 3. Therefore, some Al, Cu, Fe and Ni alloys are prone to liquid metal embrittlement [24] during FIB irradiation.

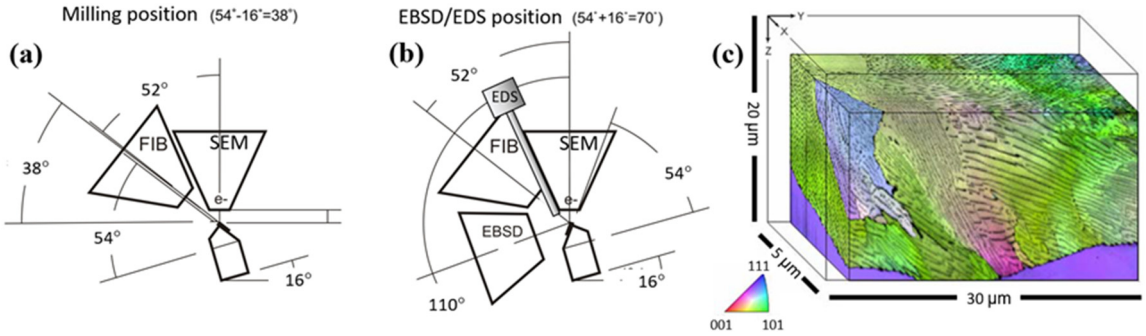

Figure 2. Automation of FIB-SEM EBSD and EDS. a) Schematics of FIB milling geometries. b) Schematics of EBSD/EDS data collection geometries. c) 3D EBSD volume is showing microstructure of perlite block. The colour is composed of image quality (gray value) and a colour code for the crystal direction parallel to the x-axis of the sample, after [20].

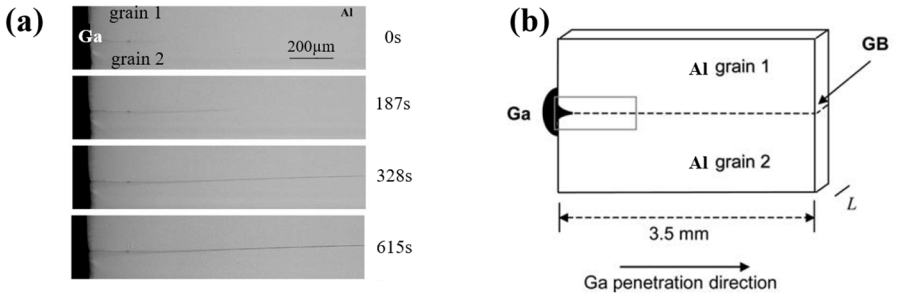

Figure 3. a) Synchrotron radiation X-ray microradiographs show continuous penetration and thickening of Ga along an Al grain boundary. b) Schematic drawing of the Al bicrystal in contact with the Ga droplet. The bicrystal has a grain boundary length of 3.5 mm and a width L of 0.8 mm [21].

b) LMIS is divergent ion source (Fig. 4a) emitting a beam shaped and focus to a spot by a FIB column. This limits the optimal beam shape and the maximum current density that is achieved by a FIB column. Therefore, usable beam shapes, beam spot sizes, and beam current densities are limited to beams having currents < 65 nA [25], see Fig. 4c. These constrain the maximum material removal rate (e.g., 17.6 $\mu m^3/s$ for Si [26]) and the maximum volume of material (for most of the materials < 50 × 50 × 50 μm^3, e.g. Fig. 2c) that is removed with reasonable amount of time.

In situ gas injection systems (GIS) have added site-specific matter deposition, micrometre-size complex structure fabrication [28, 29], and enhanced milling/etching functionalities [17]. While nano-manipulators together with GIS have enabled micro-scale sample preparation, manipulation and transfer, e.g., TEM lamella [30] and atom probe tomography (APT) [31], nano-pillars extraction, preparation and lift-out [17].

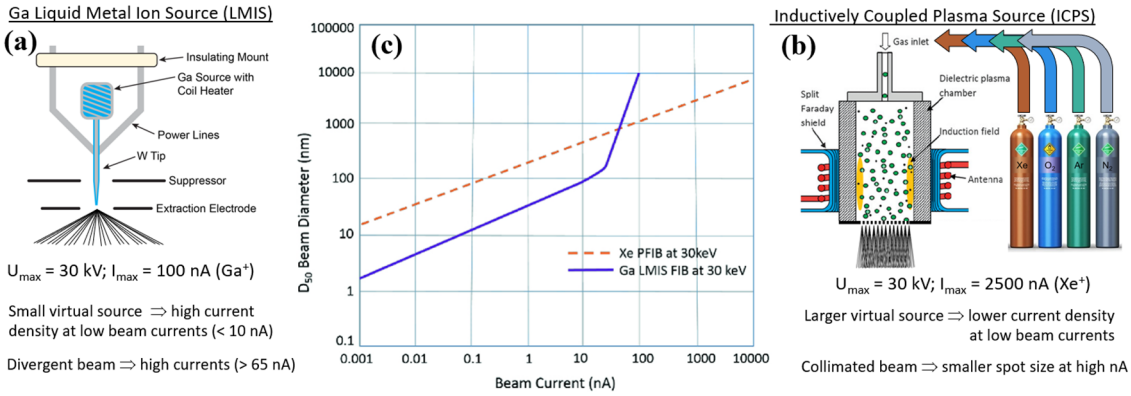

Figure 4. a) Schematics of liquid metal ion source. b) Schematics of inductively coupled plasma source. c) Comparison of the beam diameter versus the ion beam current for LIMS and ICPS based FIB columns [27].

FIB-SEM equipped with cryogenic stage kits are suitable for milling and imaging of untreated biological and beam sensitive specimens [32]. In Life Sciences, cryo FIB-SEMs are preparing samples for cryo electron correlative microscopy and tomography workflows [33].

In the early 2010's, the first experimental TriBeam systems, based on FIB-SEM platforms (Fig. 5b), femtosecond laser (chirp pulse amplified (CPA) titanium sapphire (Ti:sapphire) femtosecond lasers with approximately 150 fs pulse width and 1 kHz repetition rate), and laser optics benches were tested independently at University of California Santa Barbara (UCSB), and FEI Company (Hillsboro, Oregon) [34]. These systems had SEM, FIB, and femtosecond laser beams focussed on a coincidence point in the main vacuum chamber. From circa 2017, the FIB-SEM with a separate vacuum chamber and femtosecond laser unit (Fig. 5c) is also available commercially [35]. Although the applications envelope of fully functioning FIB-SEM is expanded to sub mm-scale, and to new capabilities, e.g., laser-induced material deposition [34], 3D large volume material characterisation, etc., the aforementioned drawbacks of FIB are still remaining [34]. Particularly, the small material volume that can be accessed with high precision FIB milling is the apparent bottleneck in many advanced scientific and industrial applications.

In order to solve the small material volume removal constraints, in 2012 the first Xe plasma FIB-SEM emerged commercially [36]. Typically, PFIB-columns use electron cyclotron resonance (ECR) [37] or inductively coupled plasma (ICP) source [38] (Fig. 4b), and xenon noble gas to generate Xe^+-ions beam. Use of ECR or ICP with heavy and inert Xe^+-ions suppress the two drawbacks of LMIS FIB-based instruments. ECR and ICP source produces broad and parallel beam, shaped, and focussed by the PFIB optics to a minimum spot sizes in dozens of nm range (pA beam currents). Although the imaging capabilities of PFIB are worse than FIB (see Fig. 4c) or SHIM, the PFIB beam profile and spot size can be precisely shaped, and control to a very high beam currents [25] (Xe^+: 2,500 nA), and current densities. As a result, it greatly

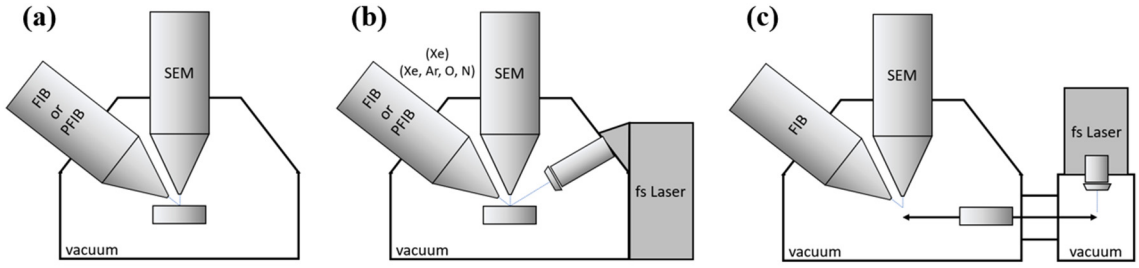

Figure 5. a) Schematics of FIB-SEM or PFIB-SEM. b) Schematics of integrated Laser FIB-SEM or Laser PFIB-SEM. c) Schematics of FIB-SEM with an external laser unit and a separate vacuum chamber.

increases the maximum material removal rate (e.g. 675 $\mu m^3/s$ for Si [26], 38× faster than for FIB), and the maximum volume of material (for most of the materials ~ 200 × 200 × 200 μm^3, e.g., Fig. 6), that can be removed with reasonable amount of time.

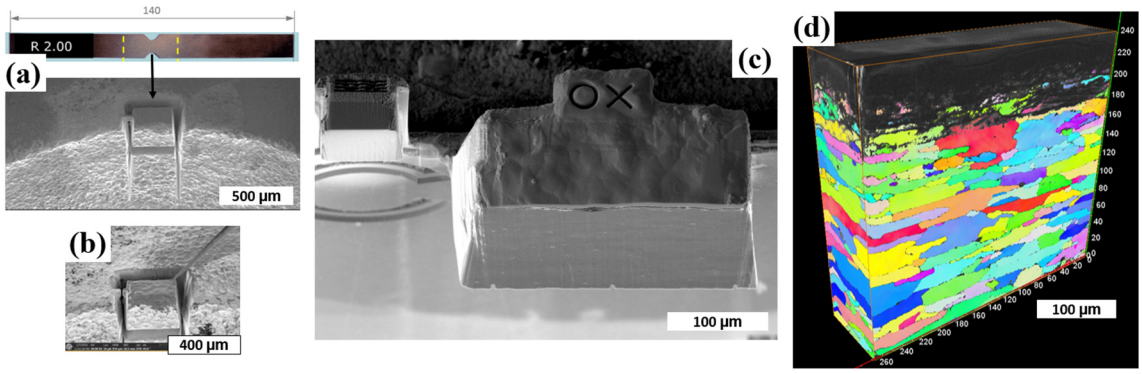

Figure 6. Large volume 3D EBSD collected using Plasma FIB-SEM [49]. a) Shot-peened double notch fatigue test 7075 sample with the material chunk ready for lift-out. b) The lift-out using EasyLift nano-manipulator; c) the material chunk attached to a Cu half-moon grid. d) 3D EBSD results (IPF-Z image stack. One of the volumetrically largest Xe^+ PFIB 3D EBSD datasets gathered to date).

Circa the year 2019, Xe^+ plasma FIB-SEM application envelope have been expanded by adding correlative microscopy (CM) holder kits/workflows [39], negative tilts for the stage, and installing three additional primary ion species for the PFIB column [40], namely argon, oxygen, and nitrogen (see Fig. 4b). The CM holder kit solution allows multi-scale, multi-modal study, and precise tracking of volume of interest from X-ray microCT to DualBeams. The negative tilts allow for mimic the broad ion beam (BIB) polishing action at glancing angles while spinning the irradiated surface. This led to a new technique called PFIB spin milling, where sub-mm surface areas are sequentially removed with nm-precision and recorded with SEM qualitative, and quantitative imaging modes [41]. Two noble (Xe and Ar) and two reactive (O and N) gasses expand the Materials Science and Life Science applications range for the plasma FIB-SEM microscope [42, 43].

In the subsequent year, the low voltage PFIB performance have been improved, allowing precise Xe^+ and Ar^+ beam polishing of TEM samples at 1 keV [44] and 500 eV [45, 46].

In the year 2019 the first commercial system has emerged that expands the TriBeam arrangement concept (Fig. 5b). The platform is equipped with monochromatic SEM and PFIB 2.0 columns, compact femtosecond laser (carbide ultra-short pulse (280 fs) laser tuned to green (515 nm) and near-infrared (1030 nm) pulses), beam shaping and scanning optics [40], and negative tilts stage. This system can prepare large lamellas for TEM/TKD (Fig. 7a), and mm-range cross-sections and serial sections, and when equipped with fast analytical detectors it probes a mm^3-large 3D EBSD information [47, 48] (Fig. 7b).

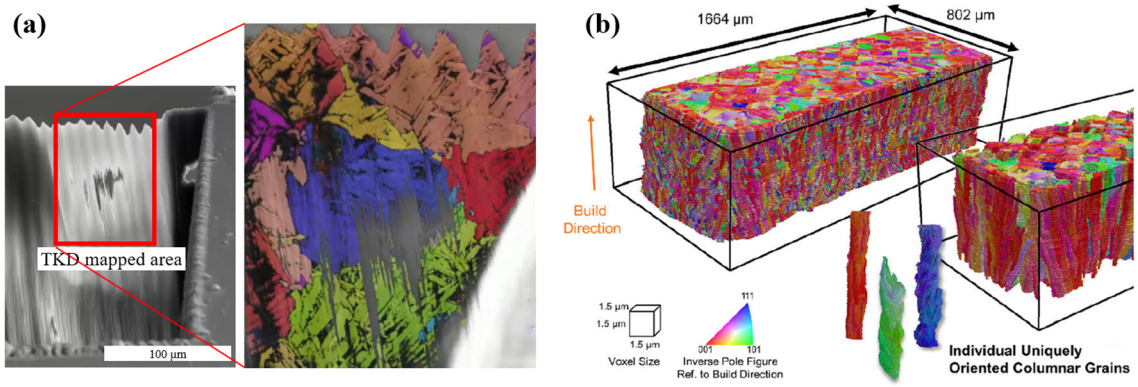

Figure 7. Helios 5 laser PFIB prepared samples. a) TKD lamella of tensile tested Ti64 alloys. Image courtesy: Dr Ali Gholinia, The University of Manchester. b) 3D reconstructions of an additively manufactured CoNi alloy sample. One of the volumetrically largest TriBeam datasets gathered to date [47].

In 2021, two additional TriBeam configurations were introduced [50] to expand the application space of these systems further. The first is a PFIB-SEM system that can use multiple primary ion species, while the second is a Ga^+ FIB SEM system. Both systems are based on the Helios 5 platform and are equipped with the same compact femtosecond laser unit as the previous configurations (similar to Fig. 5b).

3. *FOCUSSED BEAMS AND EBSD METHOD*

There are plenty of detectable and useful signals excited by a focussed electron beam in a solid matter (Fig. 8a). High energy stationary electron beam is backscattered or transmitted (electrons are transmitted through thin film or lamella, typically < 100 nm thin) from diffracting crystallographic planes of a solid volume about 20 nm deep in the crystal material. These diffracted or transmitted electrons form on a detector (phosphor screen and CCD/CMOS camera, or directly recorded with a semiconductor direct electron detector) a regular pattern of curved

bright lines, namely a backscattered Kikuchi diffraction (BKD) pattern, Fig. 8c (the traces of Kossel cones on the detector plane, Fig. 8b), or transmission Kikuchi diffraction (TKD).

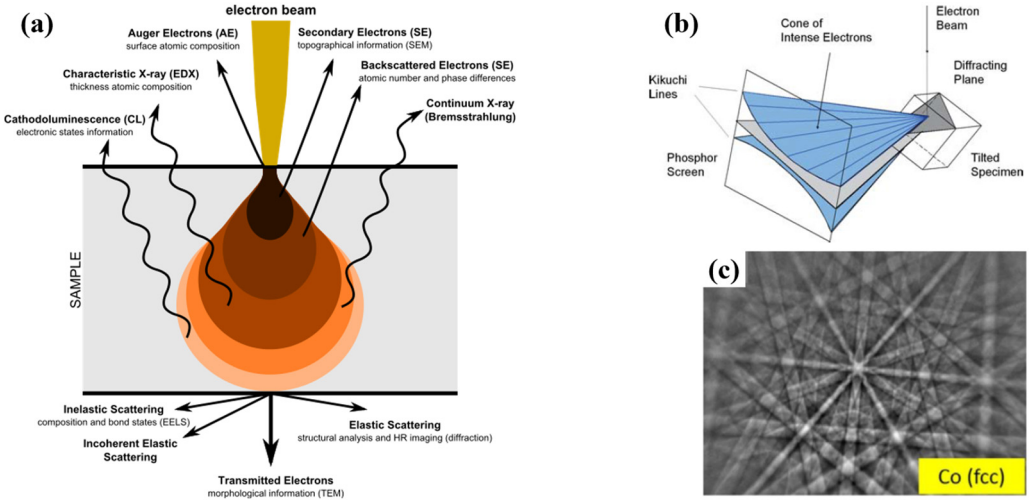

Figure 8. Interaction of focussed electron beam with a solid matter. a) Range of signals excited by an electron beam [51]. b) Schematic of the diffracting cones with respect to the reflecting plane, the specimen, and the phosphor screen [52]. c) Example backscattered Kikuchi diffraction pattern from Co grain [53].

The EBSD technique [54] (Figs. 2b and 8b and 8c) and TKD [55-57] (Figs. 9a and 9b) are standard methods to obtain spatially resolved crystallographic information via the automated analysis of Kikuchi diffraction patterns in the SEM. The onset of modern EBSD method is dated in the year 1994, when the first publication emerged on automated BKD analysis [58]. From the mid-1990's to the mid-2010's we can observe a steady increase in the number of publications that use phosphor/CCD-based EBSD technique (in practical applications of CCD-based EBSD data is collected and analysed with a speed < 1,000 fps) (Fig. 10). The introduction of commercial phosphor/CMOS-based EBSD camera systems (in practical applications of CMOS-based EBSD data collected and analysed with a speed < 2,000 fps) resulted in significant increase in the number of publications from circa 2017 (Fig. 10). In 2013, the EBSD optical path for recording Kikuchi diffraction patterns is eliminated by experimental direct electron detection (DeD) systems [59]. DeD-based detector is a compact device, thus other EBSD geometries are possible, for example tilt-free EBSD [60], (Figs. 9c to 9e). The latest development in DeD technology is electron energy-filtering detectors [61], and high-speed (~ 6,000 fps) BKD collection with the arbitrary kernel row addressing (AKRA) mode [62]. According to Scopus database [63], the first EBSD research work that uses FIB-SEM was published in 2002 [64] (Fig. 11), laser FIB-SEM in 2012 [65], PFIB-SEM in 2016 [25], and laser PFIB-SEM in 2021 [47]. Further insight to the EBSD and TKD method, various experimental setups, electron detection technology, diffraction pattern simulations, pattern matching

approaches, and the data post-processing is beyond the scope of this work. The author recommends for further reading books [52, 54], publications [52, 55-57, 59-62, 66-72], and the work cited there.

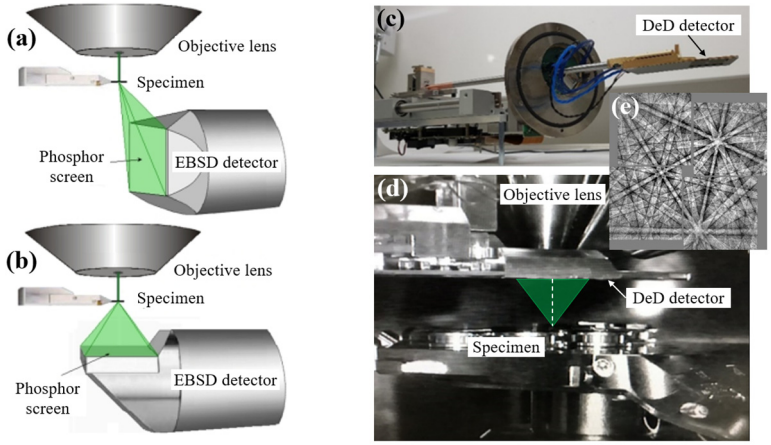

Figure 9. EBSD/TKD geometries. a) TKD using the standard EBSD camera, and b) the dedicated TKD camera [71]. An overview of the tilt-free DeD EBSD detector [60] with c) an image of the complete hardware design with electronics external to the SEM chamber, d) operational image of tilt-free geometry detector within the SEM chamber, and e) an example Ni EBSP collected in the tilt-free geometry at 20 kV with a 2 second exposure time.

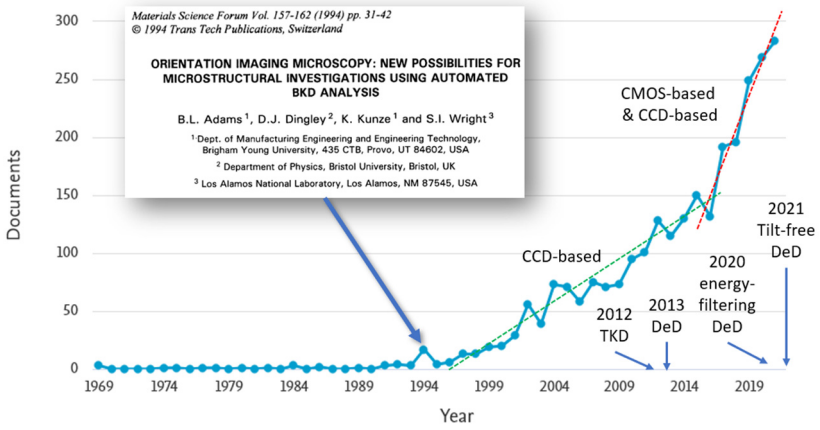

Figure 10. The graph shows number of documents published yearly on the EBSD related research, in total 2702 documents. Source: Scopus, February 2022. Search keywords: EBSD, electron backscattered diffraction, electron backscattering diffraction, backscattered Kikuchi diffraction.

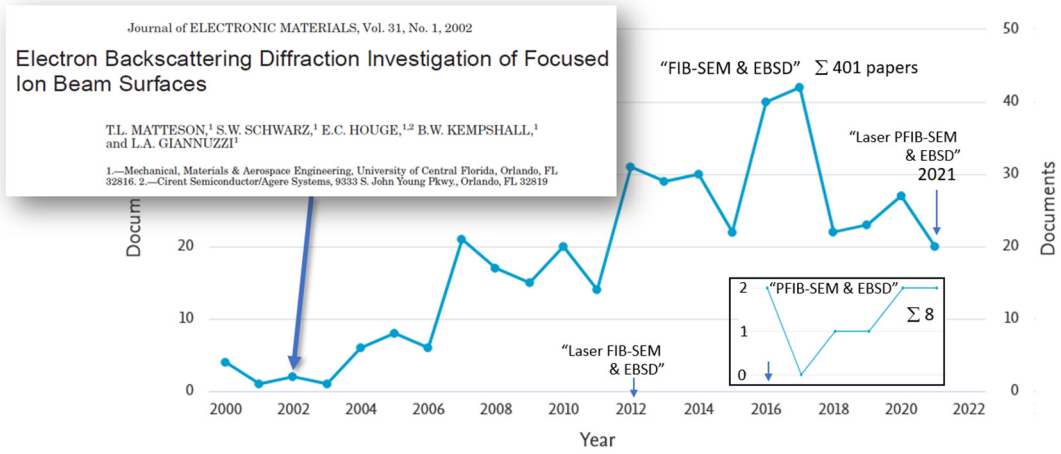

Figure 11. The graph shows number of research documents published yearly on the EBSD integrated with FIB-SEM, PFIB-SEM, laser FIB-SEM, and laser PFIB-SEM. Source: Scopus, February 2022.

4. SURFACE PREPARATION METHODS FOR EBSD

As mentioned in Section 3, Kikuchi diffraction patterns are formed by diffracted electrons travelling from the superficial layers of specimen's surface. Thus, the sample preparation methods, that retains an intact and planar at nanometre level crystalline microstructure, are critical to achieve unbiased measurements. Frequently, specimen surfaces are covered with contaminants, oxides, surface reaction products, and crystallographic scale damage induced by plastic deformations, amorphisations, heat or implantation damage. Ceramics, semiconductors, metals, and their composites, e.g., cermets, respond differently to the common sample preparation methods. Therefore, materials and specimens need to be prepared on an individual basis, and it may involve a "trial-and-error" approach.

A number of sample preparation methods for EBSD/TKD is available, and have been used [17, 30, 31, 41, 64, 65, 73-79] (these references point to one of the first papers published on the subject matter): a) metallographic grinding and polishing, b) electropolishing, c) chemical polishing, d) cleaving and fracturing, e) broad ion beam planar and cross-sectioning polishing, f) focussed ion beam planar (FIB or plasma FIB planar polishing is known as FIB/PFIB spin milling [41), cross-sectioning polishing, g) and femtosecond laser polishing. This paper gives a brief insight on methods f) and g).

4.1. Ga^+ FIB and plasma FIB

A high-energy beam of particles interacts with a solid, causing initiation of several processes in the volume of interaction [17], as depicted in Fig. 12a. When considering a focussed beam preparation of the sample surface, it is crucial to maximise: *i*) the sputtering of substrate's atoms (the maximums in Fig. 12b), and *ii*) the backsputtering of primary ions.

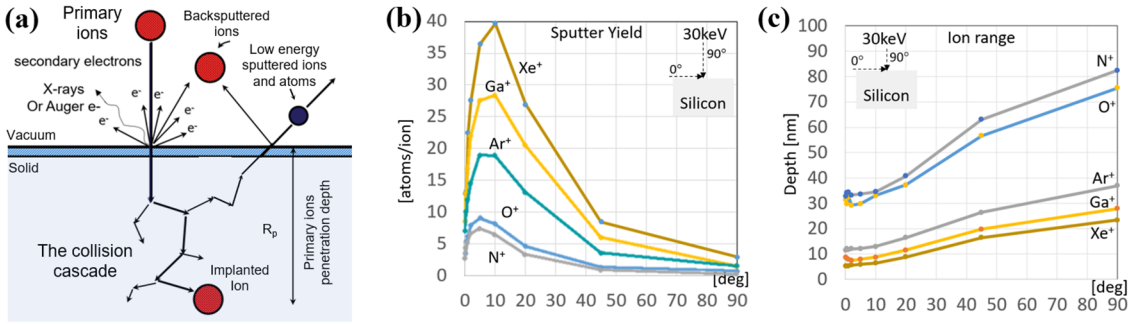

Figure 12. a) Schematic diagram of the sputtering process and ion-solid interactions (based on [80]). SRIM simulation of b) sputter yield, and c) ion penetration range of several primary ions species interacting with a silicon at various incidence angles [39].

At the same time, *iii*) the collisions induce secondary processes that need to be suppressed to a negligible level. These are: primary ions implantation (the minimums in Fig. 12b), chemical reactions, recoils of constituent atoms, defects formation, thermal and radiation-induced diffusion, mixing of constituent elements, phase transformation, amorphisation, and re-crystallisation. Further, it is important to suppress *iv*) the surface morphology changes by the ion implantation and sputtering, namely, curtains, craters, facets, grooves, ridges, pyramids formation, blistering, and exfoliations. In general, processes *i*) - *iv*) are competing phenomena. Thus, to achieve EBSD/TKD suitable surface finish the following priorities for sample preparation need to be enforced: 1) pristine surface finish and roughness at nm-range, 2) intact crystal lattices, and 3) maximum sputter yield of substrate atoms. As a result, low glancing angles (0° - 8°.) of FIB, PFIB milling and polishing, and a range of ion energies (30 keV - 500 eV) are used (Fig. 13a). PFIB may need additionally application of the rocking mill approach to mitigate surface curtains [25]. Automated 3D EBSD runs are typically performed at 30 keV and the polishing currents (FIB: 1 nA, PFIB: 60 nA). EBSD/TKD sample preparation is starting from the high ion energy (30 keV) and beam milling/polishing currents (FIB: 10 … 1 nA, PFIB: 200 … 60 nA), and finishes at very low ion energies (down to 500 eV, for FIB and PFIB) and beam currents (≥ 50 pA). SRIM [81] calculated ions ranges in silicon for Ga^+ FIB and PFIB (Ar^+, Xe^+) are similar for energies < 2 keV, but PFIB gives the benefit of gallium-free specimen preparation (Fig. 13b). Ar^+ PFIB prepared samples directly compete with Ar^+ broad ion beam polished specimens [46]. While recently, Ne^+ HIM have been used to prepare an EBSD quality Cu specimen [82].

4.2. Ultra-short pulse lasers (USPL)

In simplified terms, laser electromagnetic radiations interact only with electrons of material atoms, since nuclei are too heavy [83]. The processes vary for metals, semiconductors, and dielectrics. Figure 14 shows the timescale of electron and lattice processes in laser-irradiated solids. Femtosecond laser pulse transfers energy during carrier excitation and thermalisation, subsequent processes follow without external energy. While being close to the ablation

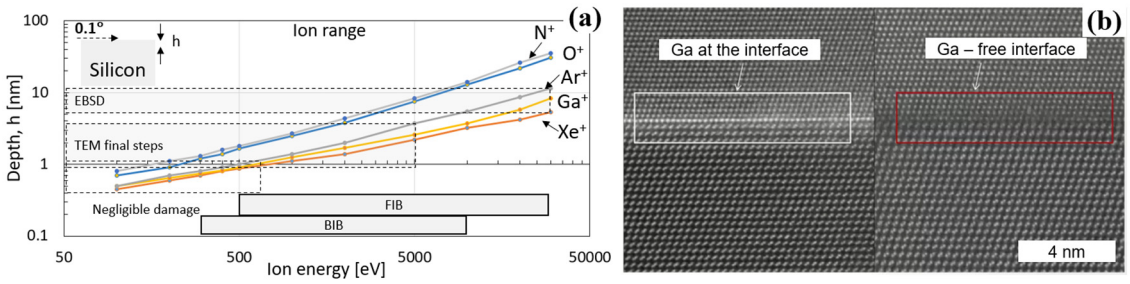

Figure 13. a) SRIM simulation of ions implantation ranges for energies 100 eV to 30 keV; 0.1 glancing angle of ions. b) Titan 300, STEM HAADF Z-contrast; Al/Si interface; Ga FIB versus Xe PFIB. Image courtesy: Brandon Van Leer and Chengge Jiao, Thermo Fisher Scientific [46].

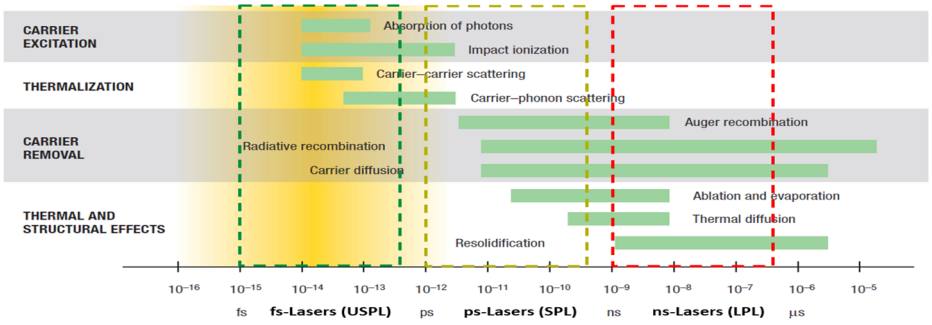

Figure 14. Timescale of electron and lattice processes in laser-irradiated solids [83].

threshold, the other thermal and structural effects are suppressed to a negligible level, allowing high quality EBSD mapping [34, 47, 65, 84, 85], see Fig. 15b, c (adopted from [84]). Very high fluences transfer so much energy causing pronounced thermal and structural effects [34, 86, 87], e.g., dislocations injection, phase transformation, amorphisation and re-crystallisation.

One of inherent features of femtosecond laser ablation of a solid in the low fluence regime is formation of the laser induced periodic surface structure (LIPSS) [84, 85], see regions A in Fig. 15b. LIPSS varies significantly with the pulse width of the laser beam, and laser processing conditions (the laser polarisation, repetition rate, laser fluence, laser scanning patterns) [47, 48]. These nano-sized structures retain the original crystalline lattice with negligible lattice damage (see Fig. 7a) have the periodicity in the range of half of the laser wavelength, and the roughness in the range of dozens of nanometres. LIPSS may obscure the diffracted electrons leading to non-indexed areas on the surface (Fig. 16a). However, tedious selection of laser processing parameters can suppress LIPSS to the negligible level (Fig. 16a) [88]. Materials surfaces prone to laser damage need to be post-laser processed. For example, the surface damage and the periodic surface structure can be removed by FIB (30 keV … 5 keV, < 30 nA, < 10° glancing angle [85], Fig.16b) or PFIB (30 keV and lower, ≤ 60 nA, < 10° glancing angle [26]) polishing. Nevertheless, some materials (e.g., GaN [85]) are more sensitive to FIB induced damage than damage generated by fs-laser ablation, leading to reduced quality of recorded Kikuchi patterns.

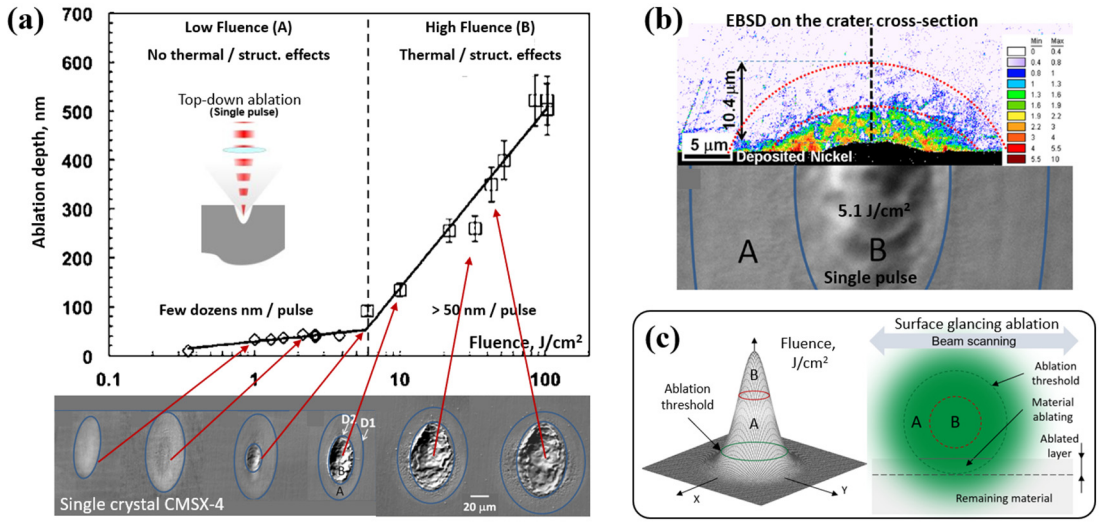

Figure 15. Femtosecond laser interaction with matter. a) The ablation depth versus the laser fluence for CMSX-4 Ni-based alloy single crystal [84]. b) EBSD grain reference orientation deviation (GROD) map (in degrees) [84]. c) Schematics of laser fluence spatial profile and ablation geometry at surface glancing angles (based on [85]).

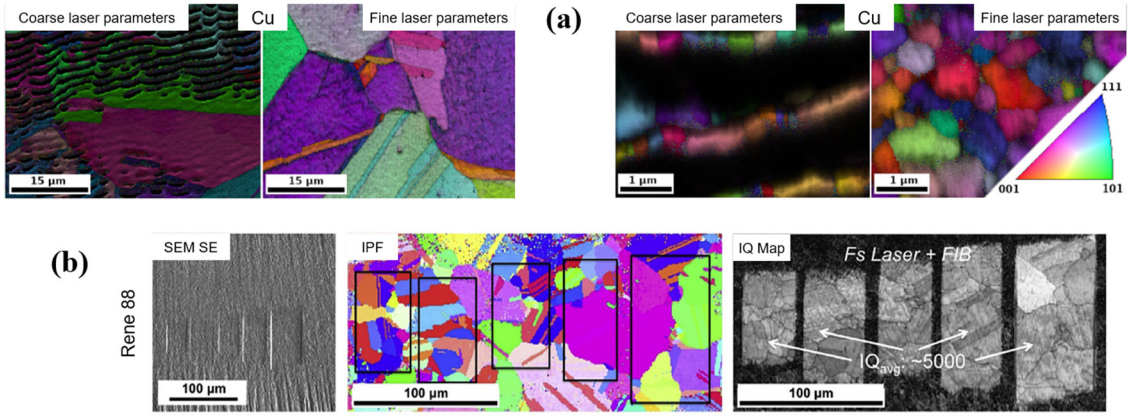

Figure 16. EBSD images (inverse pole figure with superimposed image quality). a) Coarse grain copper (left) and ultrafine grain cooper processed with a 300 fs, $\lambda = 512$ nm laser, the fluence 1.96 J/cm^2, the repetition rate 37.5 kHz for coarse, and 12.5 kHz for fine laser parameters [88]. b) Rene 88 machined with 150 fs, $\lambda = 780$ nm laser with 1 kHz repetition rate, and FIB polished at 30 keV, 20 nA [85].

5. *CONCLUSION AND FURTHER DIRECTIONS*

This paper briefly reviews the last 30 years of the development of the focussed beams (electron, ion, and photon beams) and their application for the EBSD and TKD methods. In the beginning, these beams formed standalone research platforms. The development of FIB-SEM microscope opened up *in situ*, and site-specific investigation in the micro- and nano-scale, and in two- and three-dimensions. Improved beams performance, various electron detection channels and

analytical detectors (EBSD, EDS, WDS, etc.) add new imaging modalities and quantitative analyses possibilities. Xenon plasma FIB expands the application space, and increases 3D EBSD material volume analysed with DualBeams. EBSD and EDS data mapping remain the slowest part of the 3D data collection workflow, although there are exciting improvements in detector speed with DeD EBSD. Multi-ion plasma beam and low keV beam performance further expands the application spaces of PFIB to a) a broader range of life sciences applications (with oxygen beam), and b) near damage-free surface preparation (with argon and xenon beams). The recent addition of femtosecond laser beam to the Helios 5 DualBeam microscope platforms enables the collection of high-quality 3D EBSD datasets in the mm^3-volume range at sub-micrometre SEM imaging resolution. Athermal femtosecond laser serial sectioning of soft polymers and biological materials, as well as integrated circuit devices, demonstrates good surface quality and finish. PFIB-SEM and laser PFIB-SEM becoming an essential part in the multi-modal CM workflows, being the essential link between the macro- and nano-scale. The envisaged advancement of CM workflows, on-the-fly data reconstruction, smart sampling, active prior knowledge analysis and instrument feedback, as well as additional imaging modalities, will expand the already broad application envelope of the focussed beams.

6. REFERENCES

[1] Ruska E 1986 *Applied Optics* **25** 820

[2] Hawkes P W 1985 *The beginnings of electron microscopy*. (Hawkes P W; Ed.) [London: Academic Press]

[3] Von Ardenne M 1939 *Improvements in electron microscopes*. Pattent GB511204A [UK]

[4] McMullan D 1995 *Scanning* **17** 175-185

[5] Krohn V E and Ringo G R 1975 *Appl. Phys. Lett.* **27** 479-481

[6] Orloff J 1996 *J. Vacuum Sci. Technol. B* **14** 3759

[7] Jun-ichi Nishizawa M J A 2009 *Proc. Jpn Acad. Ser. B: Phys. Biol. Sci.* **85** 454-465

[8] Schawlow A L and Townes C H 1958 *Phys. Rev.* **112** 1940

[9] Sooy W 1965 *Appl. Phys. Lett.* **2** 36-58

[10] Goldstein J, *et al.* 2017 *Scanning electron microscopy and X-ray microanalysis*. [Berlin-Heidelberg: Springer-Verlag]

[11] Hawkes P W and Spence J C H (Eds.) 2019 *Springer handbook of microscopy*. [Berlin-Heidelberg: Springer]

[12]. Zeiss C 2008 *Carl Zeiss SMT ships world's first ORION helium ion microscope to U.S. National Institute of Standards and Technology*. [cited 2008 July 17]

[13] GlobeNewswire 2011 *FEI announces new Vion PFIB system for advanced IC packaging. 2011*. [cited 2011 June 13]; Faster material removal opens new markets for failure analysis in advanced integrated circuit packaging applications.

[14] Knuffman B, Steele A V and McClelland J J 2013 *J. Appl. Phys.* **114** 044303

[15] Pilz W, *et al.* 2019 *J. Vacuum Sci. Technol. B* **37** 021802

[16] Bassim N, Scott K and Giannuzzi L A 2014 *MRS Bull.* **39** 317-325
[17] Yao N 2010 *Focussed ion beam systems, basics and applications*. [Cambridge, MA: Cambridge University Press]
[18] Feng Q, *et al.* 2005 *Scripta Materialia* **53** 511-516
[19] Williams J. 2014 *The dual-beam - Its birth, progress, and future*. in: Microscopy Today, July 2014
[20] Zaefferer S, Wright S I and Raabe D 2008 *Metallurgical Mater. Trans. A: Phys. Metall. Mater. Sci.* **39** 374-389
[21] Ludwig W, Pereiro-López E and Bellet D 2005 *Acta Materialia* **53** 151-162
[22] Lu N, *et al.* 2021 *Acta Materialia* **217** 117145
[23] Hugo R C and Hoagland R G 1998 *Scripta Materialia* **38** 523-529
[24] Lejcek P, Sob M and Paidar V 2017 *Progress Mater. Sci.* **87** 83-139
[25] Burnett T L, *et al.* 2016 *Ultramicroscopy* **161** 119-129
[26] Winiarski B and Geurts R 2020 *Microsc. Microanal.* **26** (Suppl 2) S4-S8
[27] Smith N S, *et al.* 2006 *J. Vacuum Sci. Technol. B: Microelectr. Nanometer Struct.* **24** 2902-2906
[28] Jenke M G, *et al.* 2011 *Nano Letters* **11** 4213-4217
[29] Prestigiacomo M, *et al.* 2004 *Microelectr. Eng.* **76** 175-181
[30] Jacob P, *et al.* 1999 *New FIB-supported approaches for EELS-capable TEM-lamella preparation*. in: Proc. Int. Symp. Physical and Failure Analysis of Integrated Circuits (IPFA). 69-72
[31] Thompson G B, *et al.* 2003 in: *Proc. Materials Research Society Symp.* **788** 553-558
[32] Mulders H 2003 *GIT Imaging Microsc.* **2** 8-10
[33] Schaffer M, *et al.* 2015 *Bio Protoc.* **5** 1575
[34] Echlin M P, *et al.* 2015 *Mater. Characterization* **100** 1-12
[35] Pfeifenberger M J, *et al.* 2017 *Materials & Design* **121** 109-118
[36] Jiruše J, *et al.* 2012 *Microsc. Microanal.* **18** 652-653
[37] Boukari F, *et al.* 1994 *Rev. Scientif. Instrum.* **65** 1097-1099
[38] Nabhiraj P Y, *et al.* 2010 *Nucl. Instrum. Meth. Phys. Res. A: Accelerators, Spectrometers, Detectors and Associated Equipment* **621** 57-61
[39] Winiarski B, *et al.* 2019 , *Advances in multi-beam and multi-ion FIB-SEM for 3D correlative microscopy*. in: Microscopy and Microanalysis 2019 Meeting (Portland, OR)
[40] Winiarski B, *et al.* 2019 *Microsc. Microanal.* **25** (Suppl 2) 870-871
[41] Winiarski B, Rue c and Withers P J 2019 *Microsc. Microanal.* **25** 350-351
[42] Eder K, *et al.* 2021 *Ultramicroscopy* **228** 113334
[43] Wang J, *et al.* 2021 *Scientific Rep.* **11** 13162
[44] Van Leer B, *et al.* 2020 *Microsc. Microanal.* **26** (Suppl 2) 898
[45] Jiao C 2021 , *Towards "damage-free" TEM specimen preparation by focused ion beam without gallium*. in: MRS OnDemand 2021 [Material Research Society]
[46] Jiao C, *et al.* 2021 *Low energy 500 eV focused argon ion beam provided by multi-ions species plasma FIB for Material Science sample preparations*. in: Microscopy and Microanalysis Meeting 2021. [Cambridge, MA: Cambridge University Press]

[47] Echlin M L P, *et al.* 2021 *J. Materials* **73** 4258-4269
[48] Echlin M P, *et al.* 2020 *Curr. Opin. Solid State Mater. Sci.* **24** 100817
[49] Winiarski B, Withers P J and Burnett T L 2016 *Xe+ plasma FIB milling and lift-out approach for site-specific preparation of large volume blocks for 3D-EBSD.* in: Microscopy and Microanalysis Meeting 2016. (Columbus, OH) [Cambridge, MA: Cambridge University Press]
[50] ThermoFisherScientific. Commercial Announcement: Helios 5 Laser DualBeam and Helios 5 Laser Hydra DualBeam. in: Microscopy and Microanalysis Meeting 2021. [Cambridge, MA: Cambridge University Press]
[51] Claudionico 2013 *Illustration of the phenomena that occur from the interaction of highly energetic electrons with matter, also depicting the pear shape interaction volume which is typically observed in this type of interactions*. Available from:. https://commons.wikimedia.org/wiki/File:Electron_Interaction_with_Matter.svg
[52] Schwarzer R A, *et al.* 2009 *Present state of electron backscatter diffraction and prospective developments*. in: Electron backscattered diffraction in Materials Science. (Schwartz A J, et al.; Eds.) [New York, NY: Springer]
[53] Winiarski B, *et al.* 2021 *Ultramicroscopy* **226** 113315
[54] Schwartz A J, Kumar M and Adams D P 2000 *Electron backscatter diffraction in Materials Science*. [New York, NY: Kluwer Academic / Plenum Publications]
[55] Keller R R and Geiss R H 2012 *J. Microscopy* **245** 245-251
[56] Trimby P W and Cairney J M 2014 *Adv. Mater. Processes* **172** 13-15
[57] Liu J, *et al.* 2019 *Ultramicroscopy* **205** 5-12
[58] Adams B L, *et al.* 1994 *Mater. Sci. Forum* **157** 31-42
[59] Wilkinson A J, *et al.* 2013 *Phys. Rev. Lett.* **111** 065506
[60] Marshall A L, *et al.* 2021 *Ultramicroscopy* **226** 113294
[61] Bammes B and Bilhorn R 2020 *Microsc. Microanal.* **26** 1186
[62] Wang F, *et al.* 2021 *Ultramicroscopy* **220** 113160
[63] SCOPUS 2022 Keywords: FIB-SEM or FIB and EBSD. (cited 2022 28-Feb-2022). Available from: https://www.scopus.com
[64] Matteson T L, *et al.* 2002 *J. Electr. Mater.* **31** 33-39
[65] Echlin M P, *et al.* 2012 *Rev. Scientif. Instrum.* **83** 023701
[66] Winkelmann A, *et al.* 2021 *J. Microscopy* **284** 157-184
[67] Singh S, Ram F and de Graef M 2017 *J. Appl. Crystallogr.* **50** 1664-1676
[68] Foden A, *et al.* 2019 *Ultramicroscopy* **207** 112845
[69] Trimby P W 2012 *Ultramicroscopy* **120** 16-24
[70] Mingard K P, *et al.* 2018 *Ultramicroscopy* **184** 242-251
[71] Schwarzer R 2021 Transmission Kikuchi diffraction TKD. EBSD and BKD. (cited 2022). Available from: http://www.ebsd.info/tkd.htm
[72] Guyon J, *et al.* 2016 *Ultramicroscopy* **161** 161-167
[73] Echlin P 2009 *Handbook of sample preparation for scanning electron microscopy and X-ray microanalysis*. [Cambridge, MA: Springer]

[74] Katrakova D and Mücklich F 2001 *Praktische Metallographie/Practical Metallography* **38** 547-565
[75] Ajantiwalay T, *et al.* 2019 *Micron* **118** 1-8
[76] Nowell M M, Witt R A and True B W 2055 EBSD sample preparation: Techniques, tips, and tricks. *Microscopy Today* **13**(4) 44-49
[77] Wynick G L and Boehlert C J 2005 *Mater. Characterization* **55** 190-202
[78] Erdman N, Campbell R and Asahina S 2066 Precise SEM cross-section polishing via argon beam milling. *Microscopy Today* **14** 22-25
[79] Michael J R and Kotula P G 2008 *Microsc. Microanal.* **14** (Suppl 2) 976-977
[80] Giannuzzi L A and Stevie F A (Eds.) 2005 *Introduction to focused ion beam*. [New York, NY: Springer]
[81] Ziegler J, Biersack J and Littmark U 1985 *The stopping range of ions in matter*. [New York, NY: Pergamon Press]
[82] Wolff A 2021 *Microsc. Microanal.* **27** (Suppl 1) 1016
[83] Sundaram S K and Mazur E 2002 *Nature Mater.* **1** 217-224
[84] Kumar A and Pollock T M 2011 *J. Appl. Phys.* **110** 083114
[85] Echlin M P, *et al.* 2017 *Acta Materialia* **124** 37-46
[86] Gorelik T, *et al.* 2003 *Appl. Phys. A: Mater. Sci. Processing* **76** 309-311
[87] Sedao X, *et al.* 2016 *ACS Nano* **10** 6995-7007
[88] Jelinek A, *et al.* 2021 *J. Materials* **732** 4248-4257